JOURNAL DE PHYSIQUE *Colloque C 1, supplément au n° 2-3, Tome 32, Février-Mars 1971, page* C 1 - 622

EFFECTS OF HYDROSTATIC PRESSURE AND OF JAHN-TELLER DISTORTIONS ON THE MAGNETIC PROPERTIES OF $RbFeF_3$(*)

J. B. GOODENOUGH, N. MENYUK, K. DWIGHT and J. A. KAFALAS
Lincoln Laboratory, Massachusetts Institute of Technology, Lexington, Massachusetts 02173

Résumé. — Nous avons déterminé dans $RbFeF_3$ les rapports $(\Delta T_i/\Delta H_a)_p = 0{,}35$ et $0{,}19°/kOe$ $(\Delta T_i/\Delta P)_H = 0{,}18$ et $— 0{,}81°/kbar$ pour les transitions de premier ordre à $T_1 = 40$ °K et $T_2 = 87$ °K. Les chaleurs latentes correspondantes sont 0,006 et 0,04 cal/g ; les variations des volumes relatifs sont $\Delta V_i/V_i = 1{,}5 \times 10^{-6}$ et $— 22 \times 10^{-6}$. Nous expliquons l'inhomogénéité de la température de Néel, les structures crystallographiques, le ferromagnétisme faible au-dessous de T_2, ainsi que l'anisotropie magnétique cubique mesurée pour des champs supérieurs à 0,5 kOe.

Abstract. — $RbFeF_3$ exhibits first-order transitions at $T_1 = 40$ °K and $T_2 = 87$ °K. We report $(\Delta T_i/\Delta H_a)_p = 0.35$ and 0.19 °/kOe, $(\Delta T_i/\Delta P)_H = 0.18$ and — 0.81°/kbar for T_1 and T_2, respectively, corresponding to latent heats 0.006 and 0.04 cal/g and relative volume changes $\Delta V_i/V_i = 1.5 \times 10^{-6}$ and $— 22 \times 10^{-6}$. The inhomogeneity of the Néel temperature, the crystallographic structures, the weak ferromagnetism below T_2, and the cubic magnetic anisotropy in an $H_a > 0.5$ kOe are interpreted.

I. **Experimental.** — $RbFeF_3$ has the cubic perovskite structure above its Néel temperature $T_N = 102$ °K [1], but becomes tetragonal ($c/a > 1$) in the interval $T_2 < T < T_N$ [2]. For all $T < T_2 = 87$ °K, it exhibits weak ferromagnetism, the magnitude of σ_0 increasing abruptly below first-order transitions at $T_1 = 40$ °K and $T_2 = 87$ °K [3]. In the interval $T_1 < T < T_2$, the structure appears to be orthorhombic, and below T_1 it has lower symmetry, probably monoclinic [2]. Nevertheless the magnetic anisotropy for σ_0 appears cubic (easy axes are pseudocubic $< 100 >$ axes if $T_1 < T < T_2$, $<110>$ axes if $T < T_1$) in applied fields $H_a = 5$ kOe [4]. Although the dominant magnetic structure is a simple Type G antiferromagnet for all $T < T_N$ [5], Mössbauer measurements below T_2 distinguish two types of iron sites [1]. Different values for $\Delta T_2/\Delta H_a$ have been reported : 0.56°/kOe [1] and 0.125°/kOe [2], as well as a $\Delta T_1/\Delta H_a = 0.35$°/kOe [1].

We have measured the magnetic properties of $RbFeF_3$ in the vicinity of the first-order transformations as functions of both applied field and hydrostatic pressure. The powder sample used was obtained by grinding a single crystal grown by J.-R. O'Connor. The measurements were performed on a vibrating-coil magnetometer used in conjunction with a helium-gas pressure-generating unit. This system permits the direct measurement of magnetic moment while freely varying applied field, temperature and pressure [6].

Magnetization vs temperature curves were in good accord with previous measurements. In the temperature range $90 < T < 120$ °K and in fields

$$1 < H_a \leqslant 10 \text{ kOe}$$

at both atmospheric pressure and at 5 kbars, the magnetization vs temperature curves show no kink in the vicinity of T_N, which supports the conclusion of Wertheim et al. [1] that T_N varies spatially as a result of lattice strains produced by crystallographic distortions accompanying short-range magnetic order.

Hydrostatic pressure, though shifting T_1 and T_2, does not significantly change the magnitudes of the weak ferromagnetic components as a function of $(T_1 - T)$ or $(T_2 - T)$, where $T_1 \approx 41$ °K in our sample. T_1 and T_2 varied linearly with applied field and pressure in the ranges $1 < H_a \leqslant 12$ kOe and $1 < P < 6$ kbars. The resultant slopes are listed in Table I. The measured sharp increases in ferromagnetic moment $\Delta\sigma_1$ and $\Delta\sigma_2$ on cooling through T_1 and T_2 were 2.0 and 3.5 e. m. u./g. (Testardi et al [2] found 5 e. m. u./g at T_2). Substitution of these values into the Clausius-Clapeyron equations permits determination of the latent heats L_i and volume changes V_i listed in Table I. The small changes are consistent with a microscopic model for the transitions in which magnetoelastic forces play a critical role in determining the relative stabilities of the phases.

TABLE I

Parameters of the two first-order transitions in $RbFeF_3$

T_i (°K)	$(\partial T_i/\partial H)_p$ (deg/kOe)	$(\partial T_i/\partial p)_H$ (deg/kbar)	L_i (cal/g)	$(\Delta V_i/Vi)$ ($\times 10^6$)
41	0.35	0.18	.006	1.5
87	0.19	— 0.81	.04	— 22

II. **Interpretation.** — In a cubic crystalline field, octahedral-site Fe^{2+} ions have a threefold-degenerate ${}^5T_{2g,1}(t_{2g}{}^4e_g^2)$ ground state even after spin-orbit coupling has been included. At those temperatures $T < T_N$ where the spins are aligned collinearly, magnetic order insures a cooperative elastic distortion to either trigonal ($\alpha < 60°$) or tetragonal ($c/a > 1$) local symmetry [7]. These distortions do not quench the spin-orbit coupling, but introduce a very large magnetic anisotropy stabilizing the Fe^{2+}-ion spin axis parallel to the unique local axis ($g_\parallel > g_\perp$). Whether the local distortions are to trigonal or tetragonal symmetry depends on second-order considerations. Therefore, although $KFeF_3$ is rhombohedral ($\alpha < 60°$) below T_N, it is reasonable to assume that in $RbFeF_3$ the Jahn-Teller distortion is to tetragonal ($c/a > 1$) symmetry in the interval $T_1 < T < T_N$ and to trigonal ($\alpha < 60°$) symmetry below T_1.

(*) This work was sponsored by the Department of the Air Force.

In ABO_3 perovskites, distortions that optimize the anion coordination about the A cation commonly occur [8]. Although the Rb^+ ion is large enough to stabilize twelvefold coordination, which makes $RbFeF_3$ cubic above T_N, a tetragonal ($c/a > 1$) Jahn-Teller distortion reduces this coordination from 12 to (4 + 8). Additional distortions that would increase this coordination to (5 + 2 + 5) or (4 + 4 + 4) approaching ($8\frac{1}{2}$ + 4) are the orthorhombic Pbnm structure of $GdFeO_3$ [9] for the case $\mathbf{c}_O \perp \mathbf{c}_T$ and the tetragonal structure of figure 1 for the case $\mathbf{c}'_T = 2\,\mathbf{c}_T$. The

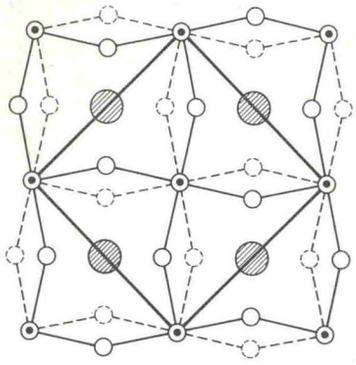

FIG. 1. — Tetragonal ($c'_T = 2\,c_T$) structure projected on the (001) plane.

orthorhombic Pbnm structure (but not the tetragonal structure) permits the existence of a Dzialoshinskii vector **D** parallel to the orthorhombic axis $\mathbf{b}_O$, and hence a canting of the Type G spin configuration to produce weak ferromagnetism. Thus the existence of a distortion to orthorhombic Pbnm symmetry below T_2 that is superposed on a tetragonal Jahn-Teller distortion in the interval $T_1 < T < T_N$ and a trigonal Jahn-Teller distortion below T_1 provides a mechanism for the appearance of weak ferromagnetism below T_2 as well as for the appearance of orthorhombic and monoclinic symmetry in the intervals $T_1 < T < T_2$ and $T < T_1$, see figure 2.

Levinstein et al. [10] have demonstrated that extensive twinning takes place below T_N, indicating

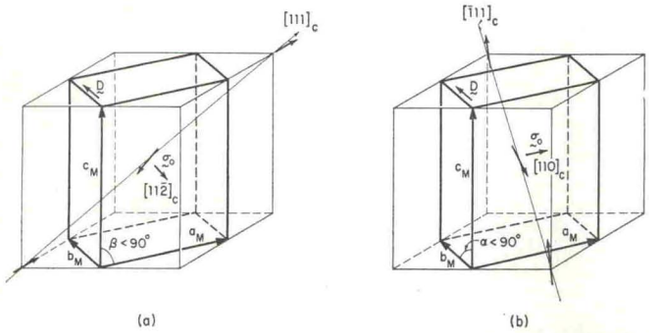

FIG. 2. — Two rhombohedral ($\alpha < 60°$) Jahn-Teller distortions superposed on the orthorhombic Pbnm structure: (a) $\beta < 90°$, (b) $\alpha < 90°$.

that strong magnetoelastic coupling is present right through T_N. This observation is compatible with dynamically cooperative Jahn-Teller distortions in regions of short-range order just above T_N, so that long-range order below T_N requires the creation of twin planes. The temperature T_N at which long-range order sets in depends upon the energy required to create twin planes for the relief of internal stresses created by the magnetoelastic coupling. In any real crystal, this energy varies from region to region, thereby leading to the spatial variation in T_N suggested by the magnetization data. Furthermore, Levinstein et al. [10] also observed directly that the ferromagnetic « orthorhombic » phase boundary moves across the twin planes of the tetragonal phase so as to include some regions having $\mathbf{c}_T \rightarrow$ « $\mathbf{c}_O$ »/2 and others having $\mathbf{c}_T \rightarrow (\mathbf{a}_O + \mathbf{b}_O)/2$. Although additional twinning occurs below T_2, the twin planes associated with the « orthorhombic » distortion are mobile in

$$H_a > 0.5 \text{ kOe} .$$

Therefore in an $H_a = 5$ kOe (where cubic torque curves were observed [4]), magnetoelastic coupling would saturate and switch the orthorhombic component of the distortion to which $\boldsymbol{\sigma}$ is coupled, but not the twinned Jahn-Teller component to which the large, antiferromagnetic spin component is coupled. (The spins are rotated by less than 2.5° in an $H_a = 16$ kOe [4].)

The direction and magnitude of the weak ferromagnetism in a crystal twinned by Jahn-Teller distortions but with a unique orthorhombic component can be obtained by minimizing $\mathbf{D}\cdot\mathbf{S}_i \times \mathbf{S}_j$. In order to obtain an [001] easy axis in the « orthorhombic » phase, it is necessary to assume that where $\mathbf{c}_T \rightarrow$ « $\mathbf{c}_O$ »/2, the orthorhombic component of the distortion transforms to the tetragonal distortion of figure 1, $\mathbf{c}_T \rightarrow \mathbf{c}'_T/2$. This simultaneously accounts for the two different hyperfine fields below T_2 and, for $H_a = 5$ kOe parallel to **[001]**, leads to the weak ferromagnetism

$$\boldsymbol{\sigma}^O = (\sqrt{2/3})\ [\mathbf{001}]\,\sigma_0^O ,$$

where the Miller indices refer to the pseudocubic cell and σ_0 is the maximum ferromagnetism possible for the given **D**. This clearly gives the cubic magnetic anisotropy observed. Switching of the spin axis from an [001] to a [111] direction to create the monoclinic phase, only adds a set of immobile { 100 } twin planes to the original { 110 } set. If the superposed distortions are, in this phase, everywhere orthorhombic Pbnm, then from figure 2, $\mathbf{D} \parallel \mathbf{b}_M$ and either $\alpha < 90°$ or $\beta < 90°$. For $H_a = 5$ kOe parallel to **[110]**, this leads to

$$\boldsymbol{\sigma}^M = \frac{1}{4}\frac{1}{\sqrt{6}}\{[\mathbf{11\bar{2}}] + [\mathbf{110}] + [\mathbf{112}] + [\mathbf{110}]\}\,\sigma_0^M = \frac{\sigma_0^M}{\sqrt{3}}\left(\frac{[\mathbf{110}]}{\sqrt{2}}\right)$$

which also gives the cubic magnetic anisotropy observed for this phase.

Significantly $\sigma^M_{110}/\sigma^O_{100} = \sqrt{(3/2)}\,\sigma_0^M/\sigma_0^O \approx \sqrt{(3/2)}$ is in reasonable quantitative agreement with the magnetization measurements.

References

[1] WERTHEIM (G.), GUGGENHEIM (H.), WILLIAMS (H.) and BUCHANAN (D.), *Phys. Rev.*, 1967, **158,** 446.

[2] TESTARDI (L.), LEVINSTEIN (H.) and GUGGENHEIM (H.), *Phys. Rev. Letters*, 1967, **19,** 503.

[3] WANG (F.) and KESTIGIAN (M.), *J. Appl. Phys.*, 1966, **37,** 975.

[4] GYORGY (E.), LEVINSTEIN (H.), DILLON, JR. (J.) and GUGGENHEIM (H.), *J. Appl. Phys.*, 1969, **40,** 1599.

[5] WANG (F.), COX (D.) and KESTIGIAN (M.), *Bull. Am. Phys. Soc.*, 1968, **13,** 468.

[6] MENYUK (N.), KAFALAS (J.), DIWGHT (K.) and GOODENOUGH (J.), *J. Appl. Phys.*, 1969, **40,** 1324.

[7] GOODENOUGH (J.), *Phys. Rev.*, 1968, **171,** 466.

[8] GELLER (S.), *J. Chem. Phys.*, 1956, **24,** 1236.

[9] GOODENOUGH (J.) and LONGO (J.), Landolt-Bornstein Tabellen, Neue Serie III/4 a (1970, Springer-Verlag, Berlin), 126.

[10] LEVINSTEIN (H.), GUGGENHEIM (H.) and CAPIO (C.), *Trans. A. I. M. E.*, 1969, **245,** 365.